

## Development of $16\mu\text{m}\times 16\mu\text{m}$ Digital Micromirror Array Suitable for Seamless-picture Projection Display System

Dae-Hyun Kim, Jin-Wan Jeon, Koeng Su Lim, and Jun-Bo Yoon

Dept. of Electrical Engineering, KAIST, Daejeon 305-701, Korea

Tel: +82-42-869-5476, E-mail address: [dhkim@3dmems.kaist.ac.kr](mailto:dhkim@3dmems.kaist.ac.kr).

Keywords : Micromirror, microlens, microdisplay, interdigitated cantilevers

### Abstract

We have developed  $16\mu\text{m}\times 16\mu\text{m}$  digital micromirror array suitable for seamless-picture projection display system. This structure can improve the picture quality by making seamless-picture image when combined with high-fill-factor microlens array to focus lights onto the mirror center. The fabricated micromirror shows excellent dynamic performances including the resonant frequency of 400 kHz.

### 1. Introduction

For several years, light valve devices based on Micro Electro Mechanical Systems (MEMS) technology, especially micromirrors, have received much attention and have gained large market share in the microdisplay areas such as projection TVs, projectors, and cinemas [1]-[3]. However, as new microdisplay markets of portable displays are emerging and the performances of other displays such as LCD, GLV, and LCOS are rapidly improved [4]-[6], it has been strongly required to improve the micromirror performances such as fill-factor, pixel resolution, switching time, and reliability [7], [8].

From this perspective, in this paper, we have proposed a seamless-picture projection display system integrated with micromirror and microlens arrays, and also developed  $16\mu\text{m}\times 16\mu\text{m}$  digital micromirror array suitable for the proposed system. Fig.1 shows the schematic view of the proposed seamless-picture projection display system composed of the micromirror array and two sheets of high-fill-factor microlens array. Using two sheets of the microlens array, the collimated incident light is focused onto the center of the individual micromirrors, reflected without any loss in the mirror edges and gaps, then come out of the system as a collimated light again. In this way, we can achieve a seamless picture so as to improve the picture quality remarkably. In order to

realize the proposed system, we need high-fill-factor microlens array, for which lots of work are already in progress [9], [10] and the micromirrors having no center hole in the mirror plate.

Therefore, in this paper, we have focused to develop high-performance  $16\mu\text{m}\times 16\mu\text{m}$  digital micromirror array utilizing interdigitated cantilevers as a spring so that the topmost mirror plate has no center hole.

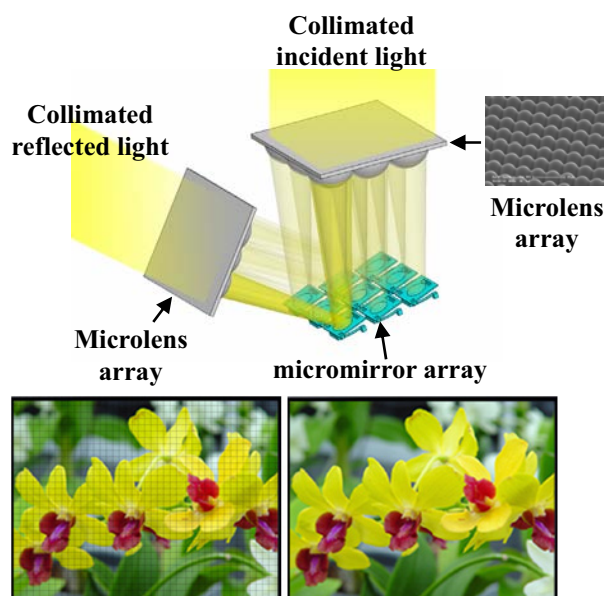


**Fig. 1. Schematic views of the proposed seamless-picture projection display system composed of the micromirror array and two sheets of high-fill-factor microlens array, and the picture quality improvement expected (left to right).**

### 2. Structure Design and Operation Principle

Fig. 2 shows the schematic view of the micromirror structure explicitly showing the unique interdigitated cantilevers and the mirror plate with no center hole.

The micromirror consists of three layers of three address electrodes, three cantilevers, and the mirror plate, respectively. Note that the cantilevers are placed in parallel but actuated toward the opposite direction with each other, so called interdigitatedly.

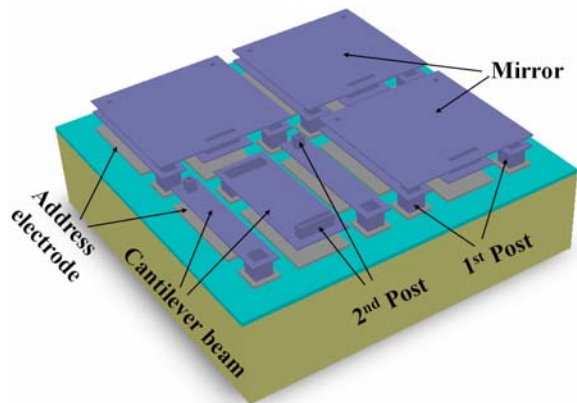


Fig. 2. A schematic view of the 2×2 micromirror array using interdigitated cantilevers

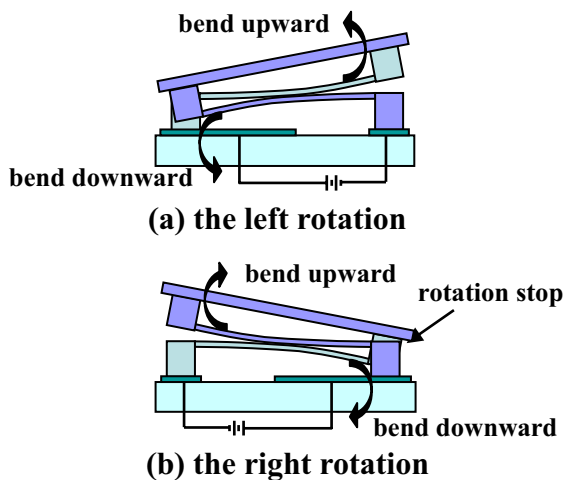


Fig. 3. Symmetrical operation principles of the micromirror using interdigitated cantilevers.

Fig. 3 shows the operation principle of the micromirror. The micromirror using interdigitated cantilevers can behave a symmetric rotation in two opposite directions through a bending actuation of cantilevers. When a driving voltage is applied in the center address electrode, the center cantilever spring is bent down, whereas the remaining outer two cantilever springs are bent up. In this way, the micromirror rotates in one direction. When a driving voltage is applied to the outer two electrodes, the mirror rotates in the opposite direction by means of the opposite reaction of the cantilevers. During symmetrical rotations of the mirror, there is no

electrical shortage if we design the height of the 2<sup>nd</sup> post smaller than that of the 1<sup>st</sup> post.

### 3. Fabrication

In this fabrication of micromirror with interdigitated cantilevers, we have used polyimide as sacrificial layer and aluminum as the material of structure to improve the thermal stability and reduce the size of mirrors differently from our previous works [10], [11].

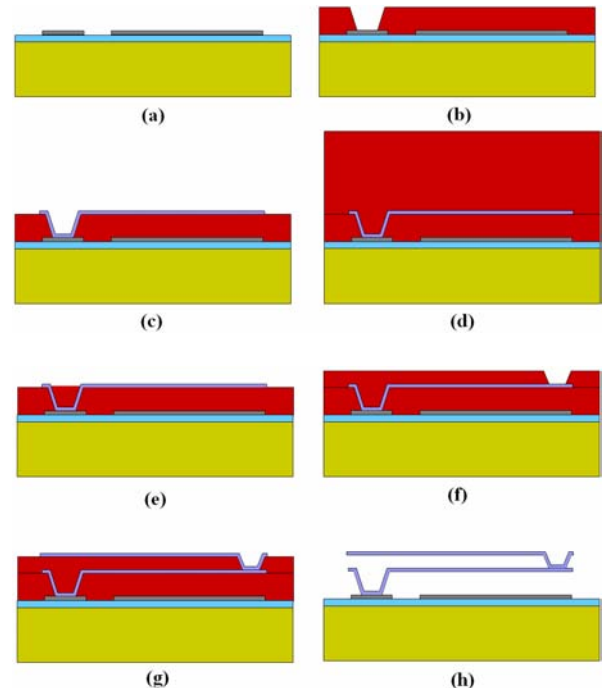


Fig. 4. Fabrication processes for the micromirror with interdigitated cantilevers: (a) bottom electrode patterning, (b) polyimide deposition and 1<sup>st</sup> post patterning, (c) cantilever patterning, (d) trench filling by polyimide, (e) etch back by plasma, (f) polyimide deposition and 2<sup>nd</sup> post patterning, (g) mirror patterning, and (h) dry release by O<sub>2</sub> plasma

The fabrication process is shown in fig. 4. Firstly, the aluminum layer with 3000Å thickness is sputtered and patterned for the bottom electrodes. Then, the 1<sup>st</sup> sacrificial layer of polyimide, PI-2555, manufactured by DuPont, is spin-coated to have a film thickness of about 2µm after curing. The cured polyimide is patterned by RIE using the plasma mixed in ratio of 90% O<sub>2</sub> and 10% CF<sub>4</sub> with a photoresist mask of 6µm in thickness for 1<sup>st</sup> post as shown in fig. 4(b). Fig. 4(c) shows the process for the interdigitated cantilever

formation that 2000Å aluminum layer is sputtered and patterned by wet etch using an aluminum etchant.

We use the trench filling and etch-back process to planarize the 1<sup>st</sup> sacrificial layer as shown in fig. 4(d), (e). Trenches with 2μm in depth in the 1<sup>st</sup> sacrificial layer are successfully filled by spin-coating of the thick-enough polyimide and proper etch-back to the aluminum layer using RIE with the plasma of 80% O<sub>2</sub> and 20% CF<sub>4</sub>. The processes for 2<sup>nd</sup> posts and the mirror are the same with those for the 1<sup>st</sup> posts and cantilevers except for the 2<sup>nd</sup> sacrificial layer thickness of 1μm. After the topmost aluminum layer is sputtered and patterned by the aluminum etchant for a mirror plate, the micromirror is dry released by O<sub>2</sub> plasma as shown in fig. 4(g), (h).

## 4. Results and Discussion

### Fabrication results

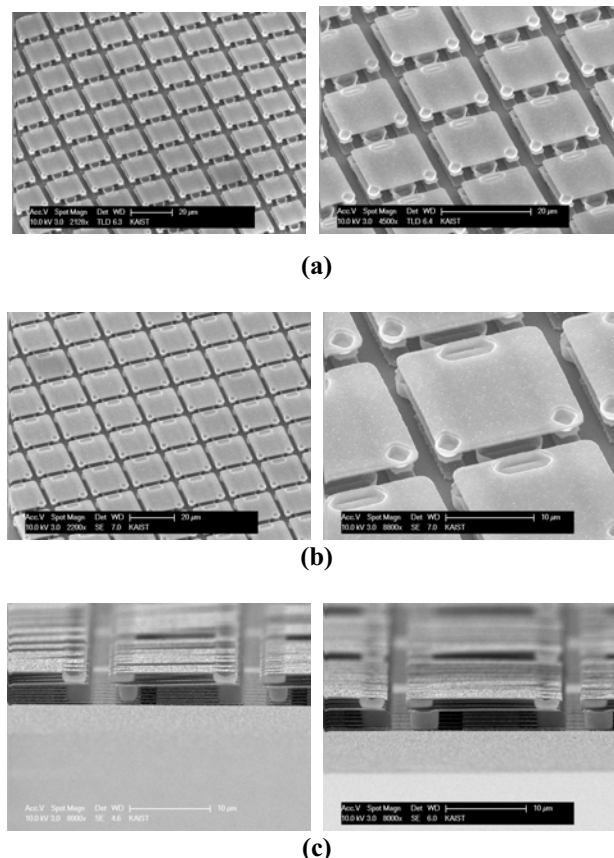
Fig. 5 shows scanning electron microscopy (SEM) images of the fabricated micromirror array with over 10×10 micromirrors. These micromirrors are made of 1<sup>st</sup> posts with 2μm thickness, cantilevers with 0.2μm thickness, 2<sup>nd</sup> posts with 1 μm thickness, and mirror with 0.2μm thickness. All of the fabricated micromirrors have flat interdigitated cantilever beams and planar mirror plates without any stress. Especially, we have obtained the planar mirror plate without topography of 1<sup>st</sup> posts through trench filling and etch back processes. Three holes remained on the mirror surface are originated from the 2<sup>nd</sup> posts.

### Measurement results

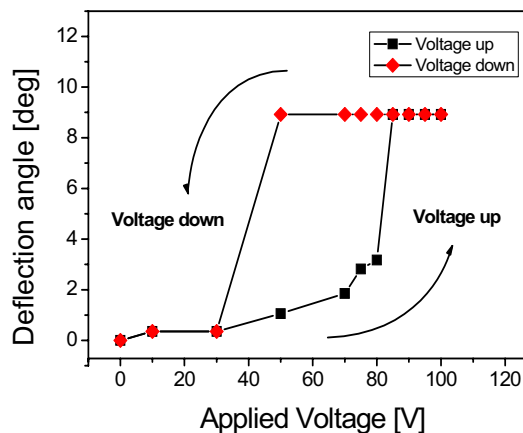
Fig. 6 shows the deflection angles of the 16μm×16μm micromirror as a function of applied voltages, which are measured by an optical surface profiler. The measured maximum deflection angle was ±8.9° at the applied voltage of 85V. The rotation angle is not increased more than 8.9° at a voltage above 85V because the 1<sup>st</sup> post played as a rotation stop (as can be seen in Fig. 3).

Fig. 7 shows the resonant frequency response of the 16μm×16μm micromirror, which is measured by Polytec Laser Doppler Vibrometer (LDV). The measured resonant frequency of the micromirror was about 400 kHz. We have gained such a high resonant frequency of 400 kHz since we used unique spring structure of three interdigitated cantilevers different from one common twisting hinge and the whole

structure is simple and light. We need to investigate later all the meaningful comparison between the interdigitated cantilevers and the common twisting hinge.



**Fig. 5. SEM images of the fabricated micromirror array: (a) top view of the 16μm×16μm micromirror array, (b) top view of the 18μm×18μm micromirror array, (c) bird's-eye view of the 16μm×16μm (left) and 18μm×18μm (right) mirrors**



**Fig. 6. Deflection angles of micromirror with 16μm×16μm size as a function of applied voltage**

Switching time responses of the fabricated  $16\mu\text{m}\times 16\mu\text{m}$  micromirror by applying step voltages of 25V in the frequency of 2 kHz is measured using LDV, as shown in Fig. 8. When the response time is defined as the time taken from 10% to 90% of maximum displacement, that of the fabricated  $16\mu\text{m}\times 16\mu\text{m}$  micromirror was measured as about 15  $\mu\text{s}$ .

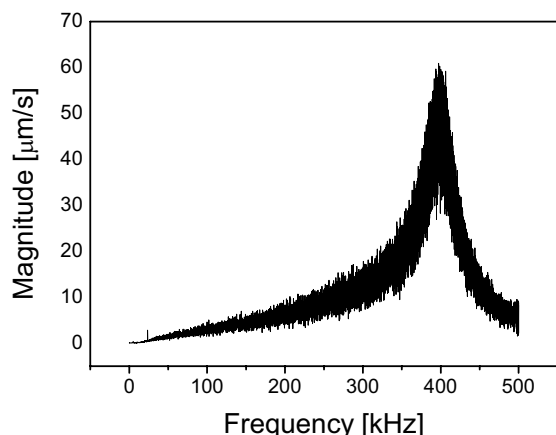


**Fig. 7. Resonant frequency responses of micromirror with  $16\mu\text{m}\times 16\mu\text{m}$  size**

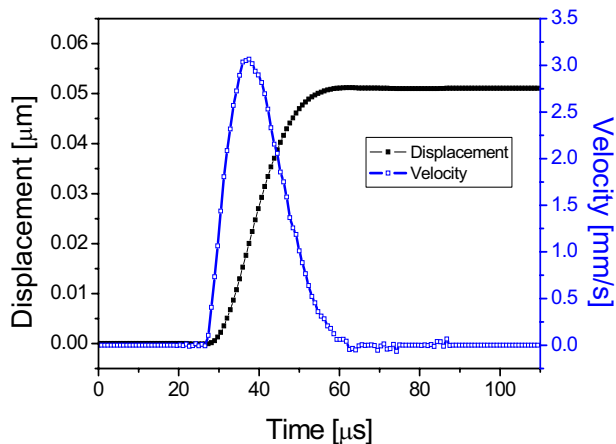


**Fig. 8. Switching time responses of the fabricated  $16\mu\text{m}\times 16\mu\text{m}$  micromirror to step function with 25V and 2 kHz**

## 5. Conclusion

The seamless-picture projection display system with micromirror array and microlens array sheets has been proposed. Also, the  $16\mu\text{m}\times 16\mu\text{m}$  micromirror using indented cantilevers have been successfully developed to meet the requirement of the proposed seamless-picture projection display system. The fabricated micromirror which does not have any

center hole in the mirror plate showed binary rotation angles of  $\pm 8.9^\circ$  at 85V. The resonant frequency was measured to  $\sim 400$  kHz and the switching response time was  $\sim 15\mu\text{s}$ .

## 6. Acknowledgement

This research was supported by a grant from the Information Display R&D Center, one of the 21st Century Frontier R&D Program, and Brain Korea 21 project, the School of Information Technology, KAIST in 2007

## 7. References

1. L. J. Hornbeck, International Electron Devices Technical Digest, 1994, pp. 381-384
2. L. J. Hornbeck, Digest of IEEE/LEOS 1996 summer topical meetings, optical MEMS and their applications, pp.7-8
3. M. A. Mignardi, Solid State Technology, 1994, vol. 37, pp. 63-66.
4. J. I. Trisnadi, C. B. Carlisle, and R. M. Micromachining and microfabrication symposium, 2004, pp.5348-05.
5. L. Banks, M. Birch, D. Krueerke, SID 2006 digest, pp. 2018-2021.
6. J. M. Teijdo, F. Ludley, O. Ripoll, SID 2006 digest, pp. 2011-2014.
7. Huffman. J., Gong. C., IEEE proceeding of BCTM, 2005, pp. 163-168,
8. A. Huibers, P. W. Richards, R. Grasser, SID 2006 digest, pp. 1618-1621
9. S.-I. Chang, and J.-B. Yoon, The 15<sup>th</sup> international conference on solid-state sensors and actuators Tech. Dig. (Transducer' 05), vol. 2, pp. 1457-1460
10. S.-I. Chang, J.-B. Yoon, Dec., 2004, Optics express, vol. 12, no. 25, pp. 6366-6371.
11. J.-W. Jeon, B.-I. Kim, J.-H. Kim, H.-K. Lee, J.-B. Yoon, E. Yoon, and K. S. Lim, the IEEE Int. MEMS Conf. Tech. Dig., 2002, pp. 528~531.
12. J.-W. Jeon, D.-H. Kim, J.-B. Yoon, and K.-S. Lim, IEEE/LEOS international conference on optical MEMS and Their Application, Oulu, Finland. pp. 53-54